

Application of ANN and RSM techniques for modeling electrospinning process of polycaprolactone

Tahere Khatti¹ · Hossein Naderi-Manesh¹ · Seyed Mehdi Kalantar²

Received: 16 June 2016 / Accepted: 4 April 2017 / Published online: 28 April 2017
© The Natural Computing Applications Forum 2017

Abstract Due to increasing application of nanofibers in many research fields, comprehensive knowledge of the electrospinning process as the most popular method of fiber production is essential. Modeling techniques are valuable tools for managing contributing factors in the electrospinning process, prior to the more expensive experimental techniques. In the present research, effective parameters on the diameter of electrospun polycaprolactone (PCL) nanofibers are analyzed using artificial neural networks (ANN) and response surface methodology (RSM). The assessed parameters include polymer concentration, voltage, and nozzle-to-collector distance. Response surface methodology based on the Box-Behnken design is utilized to develop a mathematical model as well as to determine the optimum condition for production of nanofiber with minimum diameter. In addition, multilayer perceptron neural networks are designed and trained by the sets of input-output patterns using the Levenberg-Marquardt backpropagation algorithm. The high regression coefficient value ($R^2 \geq 0.97$) and low root-mean-square error (RMSE ≤ 3.81) of the two models indicate that both models performed well in predicting PCL fiber diameter, although the RSM

model slightly outperformed the ANN model in accuracy. The represented models could assist researchers in fabricating electrospun scaffolds with a defined fiber diameter, thus specializing such scaffolds in particular applications.

Keywords Electrospinning · Nanofiber · Artificial neural networks · Response surface methodology · Polycaprolactone

1 Introduction

During the past decade, polycaprolactone (PCL) has attracted considerable attention in the biomaterial field. PCL is a semi-crystalline hydrophobic polymer, which is biodegradable and has long-term degradation. Some of the advantages of PCL are relatively inexpensive production, ease of manipulation, suitable and tailor-made physico-mechanical properties, flexibility in surface modification, and FDA approval [1]. Such special characteristics make PCL and its blends well suited for applications including tissue engineering, drug delivery, wound dressing, and fixation devices [2–5]. To date, PCL in the form of nano- and microsphere [3, 6], micelle [7], foam [8], nanofiber, and microfiber [9, 10] has been fabricated, which a nanofiber structure seems to be the most common form of PCL.

Although several available methods, such as phase separation [11] and template synthesis [12], have been developed for the fabrication of nanofibers, electrospinning has remained the most popular technique of nanofiber production. Electrospinning is the process of continuous fiber production by exploiting an electric field that affects a polymer solution or a melt extruding through a needle. Ease of use, low cost, versatility, and fiber production from many materials are some of the major advantages of electrospinning technique [13].

✉ Hossein Naderi-Manesh
naderman@modares.ac.ir

Tahere Khatti
t.khatti@modares.ac.ir

Seyed Mehdi Kalantar
kalantarsm@ystp.ac.ir

¹ Department of Nanobiotechnology, Faculty of Biological Sciences, Tarbiat Modares University, P.O. Box 14115-111, Tehran, Iran

² Department of Genetics, Research and Clinical Center for Infertility, Shahid Sadoughi University of Medical Sciences, Boo Ali Avenue, Safaiyeh, Yazd, Iran

Electrospun nanofibers are advanced materials that introduce some individual characteristics, such as large surface area, good mechanical performance, and high porosity, which are properties largely dependent on the diameter and morphology of fibers [14]. Approximation of fiber diameter before the process of electrospinning is challenging because of the complicated patterns of variables affected process output. Electrospinning variables include polymer solution factors like concentration and conductivity, along with processing parameters such as voltage, tip-to-collector distance, feed rate, and ambient condition [15]. Exploring the quantitative relationship between process variables and their output could be performed through modeling techniques.

Response surface methodology (RSM) is very popular for modeling a process and for optimization studies. RSM is a collection of mathematical and statistical techniques that are extensively applied for analyzing and optimizing processes. It determines the effect of the independent variables, alone or in combination, on the processes. The major advantage of RSM is that it minimizes the number of experiments required for statistically analyzing a process with multiple factors. In this modeling approach, polynomials are applied as local approximation; subsequently, a mathematical equation expressing the relationship between the response and the independent variables is created [16].

Furthermore, artificial neural networks (ANN), a modeling tool for solving linear and nonlinear multivariate regression problems, have also been broadly applied for modeling different kinds of processes, such as electrospinning and fabrication of composites [17–20]. This modeling technique is inspired by the biological brain. In ANN's first step, a neural network composed of two or more layers with a defined number of artificial neurons in each layer is created. A simple artificial neuron has two key components: weight and transfer function. The weight of an input is multiplied by the input units, and the weighted input is introduced to the neuron transfer function to estimate the output. In the next step, by using several input-response data points, the network is trained to approximate the relationship between the two sets of values. In the training approach, the mean square error (MSE) of experimental and predicted outputs is minimized by continuously adjusting the weights between neurons. Validating and testing the data sets, which are necessary steps for exploring the network performance, are the final steps of ANN modeling [21].

In recent years, several studies have focused on the analysis of electrospinning process using RSM and ANN. Table 1 shows the summary of researchers' studies on modeling of electrospinning aimed at predicting the diameter of nanofiber. Although several polymers have been studied thus far, no attempt has been made to model electrospinning process of PCL nanofiber, which is

Table 1 Summary of studies in modeling of electrospinning process to predict nanofiber diameter

Nanofiber	Method	Reference
Polyacrylonitrile	RSM, ANN	[18, 22, 23]
Polymethyl methacrylate	RSM, ANN	[24, 25]
Polyethylene oxide	ANN	[26]
Polyurethan	RSM, ANN	[27]
Titanium dioxide	RSM, ANN	[28, 29]
Nylon-6,6	ANN	[30]
Carbon	RSM	[31]
Poly(D,L-lactide)	RSM	[32]
Gelatin	ANN	[33]
Gelatin/cellulose acetate	ANN	[34]
Polycaprolacton/gelatin	RSM	[35]
Poly(vinyl alcohol)/chitosan	ANN	[36]
Chitosan/polyethylene oxide	ANN	[37]
Chitosan/polylactide	RSM	[38]

widely used in biomedical applications. The fiber diameter has a major role in the mechanical properties and porosity of the PCL scaffold as well as in attachment and proliferation of cells on the scaffold [39].

In the present study, two modeling techniques are employed to describe the nonlinear effect of selected electrospinning factors on the diameter of PCL, which is one of the most utilized polymers in biomaterials research. The assessed parameters of electrospinning are polymer concentration, voltage, and tip-to-collector distance. During this study, different conditions of fiber production are evaluated using the Box-Behnken design (BBD) method. Subsequently, the relationship between the diameter of polymer fibers and the above-mentioned factors is analyzed using RSM and ANN methods. Additionally, the two proposed models are compared and discussed in this paper.

2 Materials and methods

2.1 Materials

PCL (Mw = 80,000) and chloroform were obtained from Sigma-Aldrich, and *N,N*-dimethylformamide (DMF) was purchased from Merck.

2.2 Preparation of PCL solution

PCL was dissolved in a chloroform/DMF solution (9:1) at concentrations of 8, 10, and 12%. Each solution was stirred via magnetic stirrer for 3 h.

2.3 Electrospinning setup

Electrospun PCL scaffolds were fabricated using an electrospinning device (Nanoazma Co., Tehran, Iran). The prepared solution was extruded from a 5-ml syringe attached to a 21-G blunted needle. The feed rate was 0.5 ml/h, and a speed of 100 RPM was selected for collecting fibers. The electrospinning was performed at 25 °C. After electrospinning, the fibrous mats were dried for 48 h. Other electrospinning parameters to prepare different samples according to the Box-Behnken method are summarized in Table 2.

2.4 Characterization

The morphology of electrospun fibers was assessed by scanning electron microscope (SEM; TESCAN, Brno, Czech Republic) at an accelerating voltage of 30 kV under magnification of $\times 1500$ after sputter coating with a gold sputter coater. The average fiber diameter was measured from the SEM micrographs using ImageJ2 software (maintained by C. Rueden on GitHub). Fifty fibers in each sample were measured. A typical SEM photograph of the electrospun nanofiber mat and its corresponding histogram of fiber diameter distribution are shown in Fig. 1a, b.

2.5 Design of experiments

In this study, the selected design of experiments (DOE) was RSM coupled with Box-Behnken design. Among different types of DOE methods, Box-Behnken design has maximum efficiency and needs fewer experiments when three factors with three levels are involved [40, 41].

The initial step in the RSM study is the determination of the input parameters and their levels. This step was performed applying previous reports [38, 42]. Based on the literature, three independent variables were detected as more effective parameters on PCL fiber's diameter, including concentration, voltage, and needle-to-collector distance. In addition, the range of each variable was defined in such a way to produce PCL fiber with no bead.

Since the parameters have different units, the factors were first normalized according to Eq. 1:

$$x = \frac{x - (x_{\max} + x_{\min})/2}{(x_{\max} - x_{\min})/2} \quad (1)$$

where x is the coded variable, x is the natural variable, and x_{\max} and x_{\min} are the maximum and minimum values of the natural variable. Each of the coded variables is forced to range from -1 to 1 . The resultant coded and actual values are listed in Table 2.

Table 2 Actual and coded values of the selected parameters

	Coded value		
	-1	0	1
A. Concentration (% w/v)	8	10	12
B. Voltage (kV)	15	18	21
C. Tip-to-collector distance (cm)	8	10	12

Then a three-level, three-variable Box-Behnken design was performed and, consequently, 17 experiments were obtained, as shown in Table 3. The number of required experiment is given by:

$$N = 2k(k-1) + C_0 \quad (2)$$

where N , k , and C_0 are the number of experiments, variables, and center points, respectively.

The statistical software Design-Expert® (trial version of v. 7.0.0, Stat-Ease Inc., Minneapolis, MN, USA) was utilized for the design and regression analysis of the experimental data and for plotting the subsequent graphs.

2.6 Artificial neural network

In this study, multilayer perceptron ANN with two hidden layers and one output layer according to Kolmogorov's theorem was applied [43]. To achieve the optimum topology of the network, different numbers of hidden layers and neurons were examined using a trial and error approach. The optimal structure was obtained based on the lowest value of MSE and the highest correlation coefficient (R) of the data set.

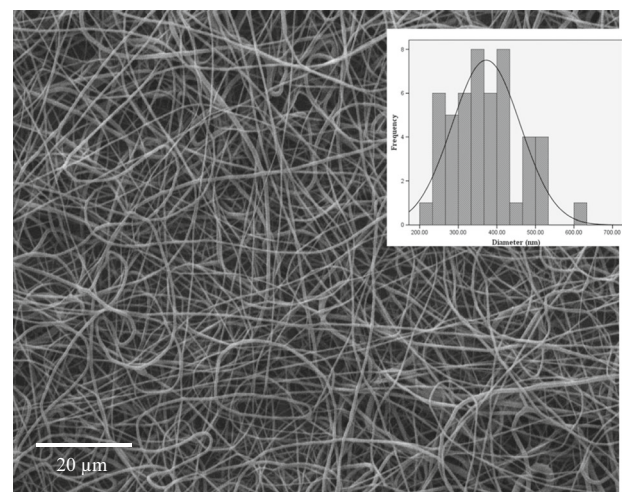


Fig. 1 SEM micrograph of electrospun PCL nanofibers and their diameter distribution

Table 3 Experimental conditions designed by Box-Behnken design and corresponding responses

Sample	Coded value of A	Coded value of B	Coded value of C	Response Fiber diameter (nm)
1	0	0	0	324
2	1	0	1	402
3	1	0	-1	485
4	-1	-1	0	127
5	1	1	0	397
6	-1	1	0	197
7	-1	0	-1	191
8	0	1	1	372
9	0	0	0	314
10	-1	0	1	320
11	0	0	0	317
12	0	-1	-1	287
13	0	0	0	324
14	0	-1	1	298
15	1	-1	0	359
16	0	0	0	313
17	0	1	-1	348

A polymer concentration, B applied voltage, C tip-to-collector distance

Among the algorithms that have been recommended for learning MLP networks, back propagation (BP) in conjunction with the Levenberg-Marquardt method was selected. BP is the fastest algorithm, although it requires more memory than the others [43]. The hyperbolic tangent sigmoid transfer function and the linear transfer function were employed for the hidden layers and output layer, respectively (Eqs. 3 and 4).

$$f(x) = \frac{e^x - e^{-x}}{e^x + e^{-x}} \quad (3)$$

$$g(x) = x \quad (4)$$

The experimental data were randomly divided into three groups, including training, validating, and testing sets, containing 70, 15, and 15% of the samples, respectively. All experimental data were normalized before ANN modeling. The calculations were performed in MATLAB mathematical software (v. 7.1) using the ANN toolbox.

In order to compare the adequacy of ANN and RSM models, the R^2 , root-mean-square error (RMSE), model predictive error (MPE(%)), and mean absolute error (MAE), were calculated according to Eqs. 5 to 8:

$$R^2 = \frac{\sum_{i=1}^n (Y_{io} - Y_{ip})^2 - \sum_{i=1}^n (Y_{io} - Y_{ip})}{\sum_{i=1}^n (Y_{io} - Y_{ip})^2} \quad (5)$$

$$\text{RMSE} = \sqrt{\frac{\sum_{i=1}^n (Y_{io} - Y_{ip})^2}{n}} \quad (6)$$

$$\text{MPE}(\%) = \frac{100}{n} \sum_{i=1}^n \left| \frac{Y_{io} - Y_{ip}}{Y_{ip}} \right| \quad (7)$$

$$\text{MAE} = \frac{1}{n} \sum_{i=1}^n |Y_{io} - Y_{ip}| \quad (8)$$

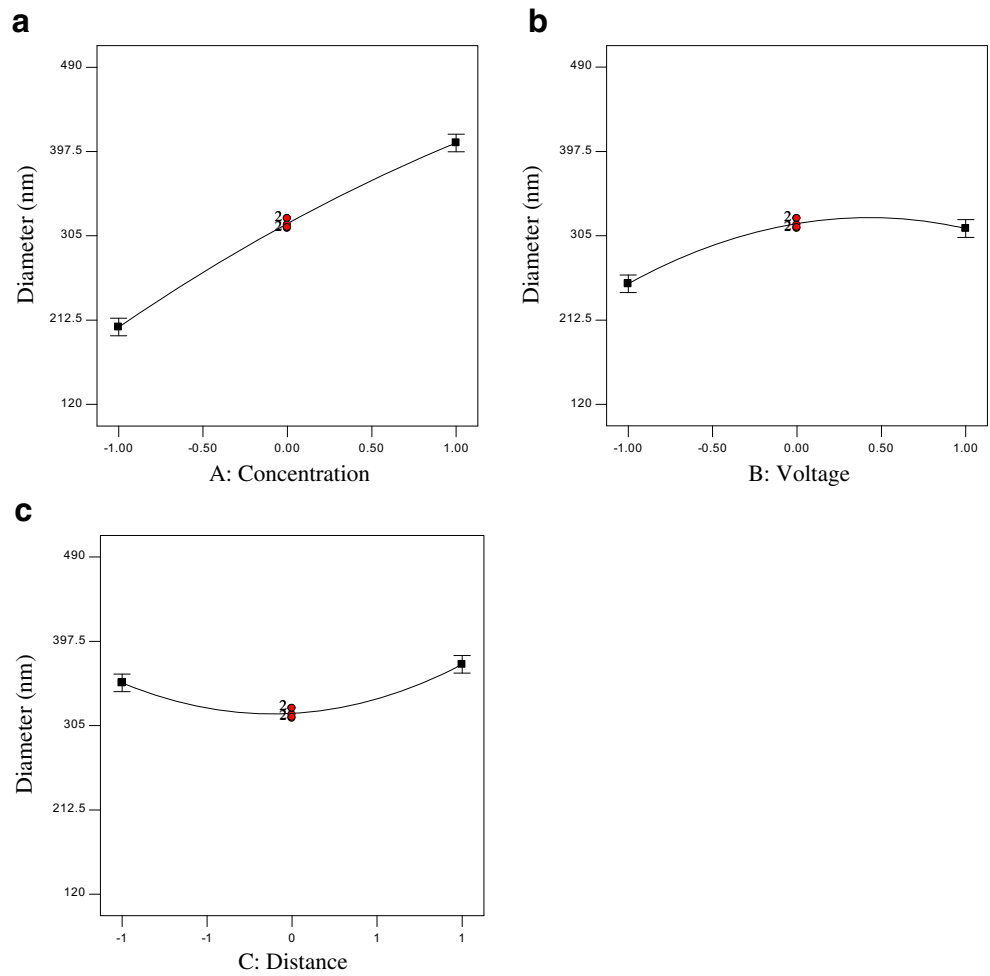
where Y_{io} and Y_{ip} are the observed and predicted values of fiber diameter and n represents the number of experiments.

Table 4 Analysis of variance (ANOVA) for response surface quadratic model of PCL fiber diameter

Source	Sum of squares	df	Mean square	F value	Prob. > F
Model	1.144 e^5	7	16,349.54	161.75	<0.0001*
A	81,608	1	81,608	807.38	<0.0001*
B	7381.13	1	7381.13	73.02	<0.0001*
C	820.13	1	820.13	8.11	0.0191*
AC	11,236	1	11,236	111.16	<0.0001*
A2	665.81	1	665.81	6.59	0.0304*
B2	5403.92	1	5403.92	53.46	<0.0001*
C2	8031.60	1	8031.6	79.46	<0.0001*
Lack of fit	796.5	5	159.3	5.63	0.0595**
Pure error	113.2	4	28.3		

*Significant at 95% confidence interval; **not significant at 95% confidence interval

Fig. 2 Main effects of the defined variables on PCL fiber diameter based on coded values: **a** concentration, **b** voltage, and **c** distance



3 Results and discussion

3.1 Statistical results obtained by RSM

To evaluate the experimental results, we examined multiple regression models. The best model, which fits all the design

points was a quadratic model. Analysis of variance (ANOVA) was used to estimate the variables’ effects and their interactions, as displayed in Table 4.

The significant terms of the model, as indicated in the ANOVA table, consist of A, B, C, AC, A^2 , B^2 , and C^2 , which had *P*-values less than 0.05. Other model terms showed no

Fig. 3 Effect of variables on electrospun fiber diameter in **a** 2D and **b** 3D views

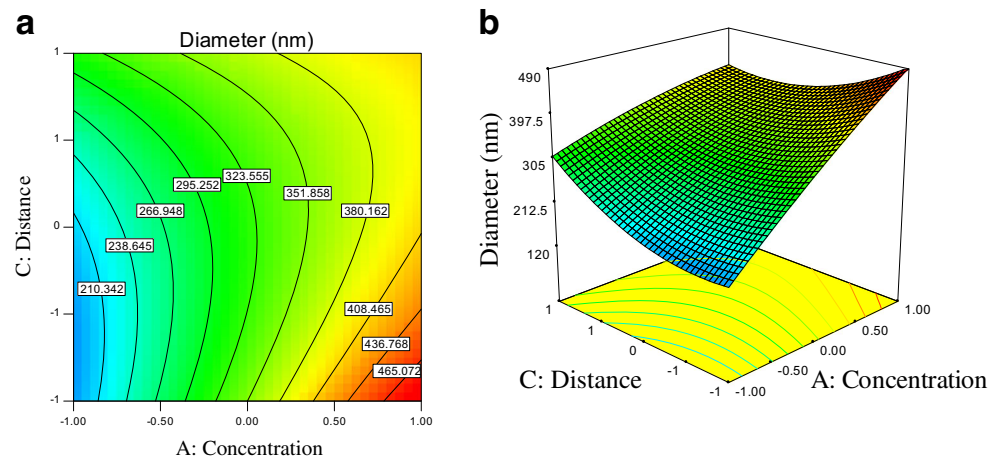
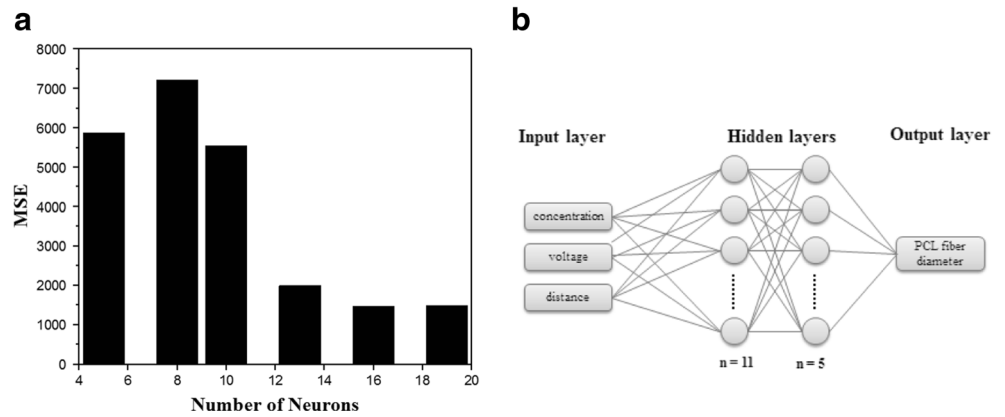


Fig. 4 Schematic view of the represented MLP network (a) and the effect of number of neurons on the performance of the ANN (b). (Note that graph (b) is obtained for one hidden layer with tansig transfer function)



significant effect on the electrospun PCL fiber diameter and thus were eliminated from the model. Afterwards, the following second-order polynomial function was determined to approximate the PCL fiber diameter:

$$Y = 318.4 + 101 A + 30.38 B + 10.13 C - 53 AC - 12.58 A^2 - 35.83 B^2 + 43.68 C^2 \quad (9)$$

where Y , A , B , and C are the average diameter of PCL fibers, coded forms of polymer concentration, voltage, and tip-to-collector distance, respectively.

As shown in the ANOVA table (Table 4), the model P value (<0.0001) and the insignificant lack of fit (0.059) implied that the experimental data have a suitable agreement with the model. Additionally, the high adjusted and predicted R -squared values, which are 0.986 and 0.949, respectively, validated the goodness of the model.

3.2 Effect of electrospinning variables on diameter

According to the ANOVA results, the response surface model clearly indicates that the most effective parameter on the PCL

Fig. 5 Regression analysis between ANN responses and the experimental results for a training, b validation, c test datasets, and d MSE plot with respect to the number of epochs for training, validation, and test samples for the PCL fiber diameter response

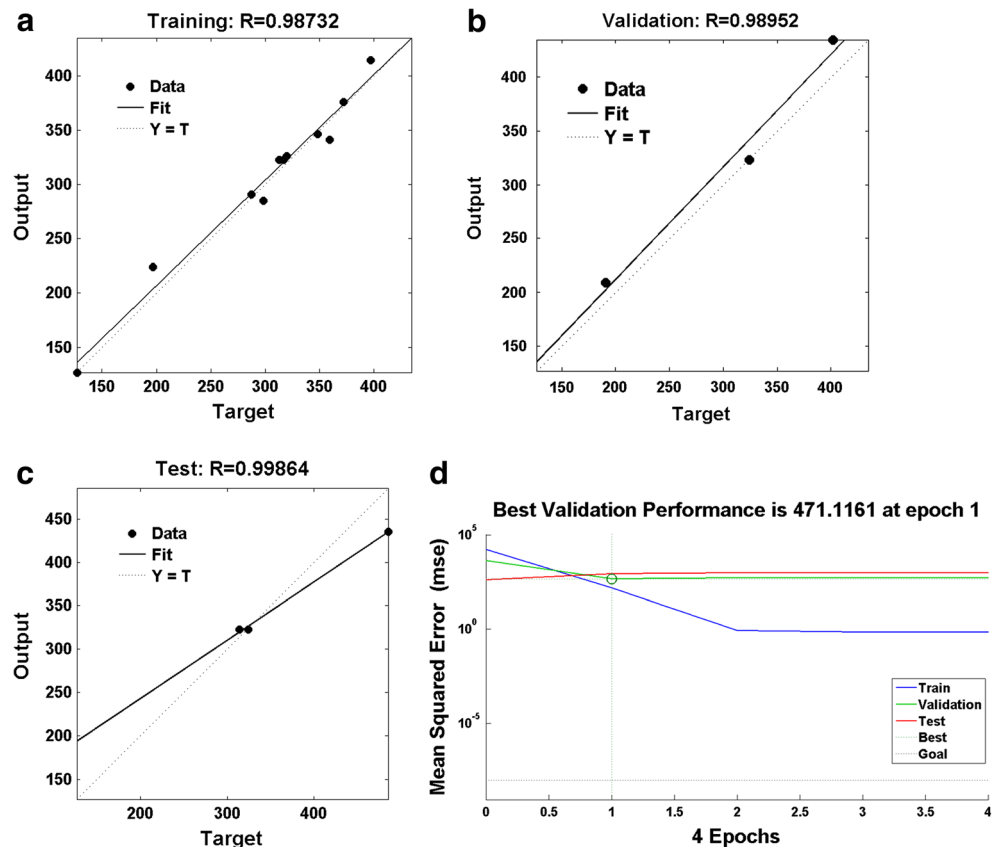
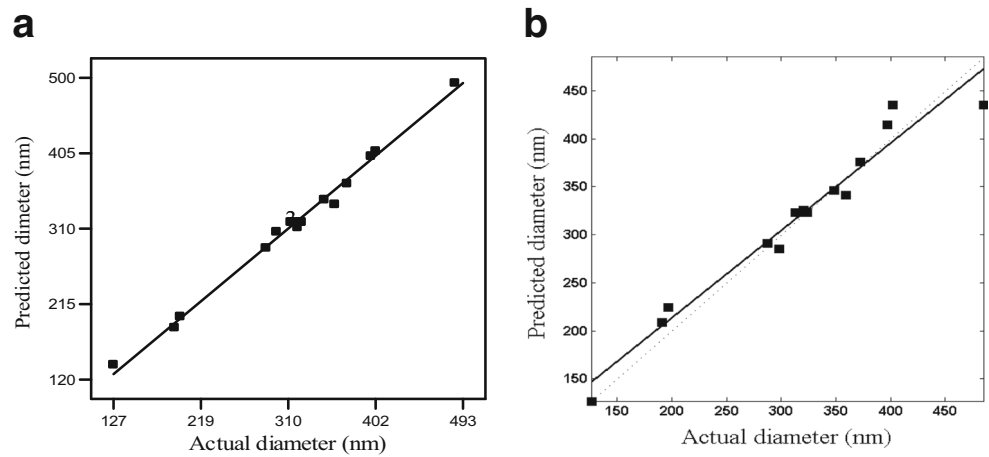


Fig. 6 Regression analysis between actual and predicted diameter of PCL fibers using **a** RSM ($R^2 = 0.984$) and **b** ANN ($R^2 = 0.970$)



electrospun fiber diameter is the polymer concentration. As corroborated in the literature, increasing polymer concentration will result in greater viscoelastic force, consequently leading to larger diameter polymer fibers [22]. The dependence between concentration and diameter, while other parameters are at their mean point, is shown in Fig. 2a. As can be seen, any change in the value of concentration is expected to lead to a significant change in the value of fiber diameter.

Table 5 Comparison between experimental and predicted values of electrospun fiber diameter by RSM and ANN models

Sample	Experimental	Predicted	
		RSM	ANN
1	324	318	313
2	402	407	363
3	485	493	490
4	127	138	132
5	397	401	398
6	197	199	160
7	191	185	164
8	372	366	368
9	314	318	313
10	320	311	270
11	317	318	313
12	287	285	290
13	324	318	313
14	298	306	302
15	359	252	314
16	313	318	313
17	348	346	349
Coefficient of determination (R^2)		0.98	0.97
Root mean square error (RMSE)		3.36	3.81
Model predictive error (%)		4.34	5.91
Mean absolute error		11.29	14.58

There is a less strong dependence between the applied voltage and diameter with a mildly increasing trend, although in the high range of voltage the trend is almost reversed (Fig. 2b).

Furthermore, tip-to-collector distance had only a mild effect on PCL fiber diameter with concave dependence (Fig. 2c). However, the interactive effect of distance with concentration is more important than its main effect. The contour plot and 3D surface plot of PCL fiber diameter at different values of concentration and distance in the middle level of applied voltage are given in Fig. 3a, b. As indicated in the contour plot, the simultaneous effect of concentration and distance on the fiber diameter is similar to conic curves, although in higher range of variables, the dependence would be stronger.

3.3 Artificial neural network results

ANNs are computational models inspired by biological nervous system. ANN includes several types such as feedforward network, radial basis function network, fuzzy network, and more [44–46]. As corroborated by Hornik et al. [43], multi-layered feedforward networks with a few as one hidden layer are capable of approximating any function from n dimensions to m dimensions to any desired degree of accuracy. Thereupon, this type of ANN was applied.

In this study, the parameter of interest is PCL fiber diameter as an output variable of electrospinning process, and three independent variables were selected as input factors, namely polymer concentration, voltage, and tip-to-collector distance. The final structure of the ANN model was obtained by examining a series of different topologies (Fig. 4a). The optimal model, determined based on the minimum value of MSE of the training and testing sets, was a three-layered perceptron feedforward ANN model with 1, 11, and 5 neurons in output, first, and second hidden layers, respectively. Figure 4b schematically illustrates the proposed ANN structure.

After creation of the network architecture through the learning process, the weights between the connections were adjusted until the optimum weights for output prediction were

Table 6 Validation study of RSM and ANN models using different levels of input variables

Sample	Values of the variables			PCL fiber diameter (nm)		
	Concentration (% w/v)	Voltage (kV)	Distance (cm)	Experimental	RSM	ANN
a	8	17	9	165	171	165
b	8	20	11	189	188	181
c	12	17	11	349	381	370

obtained or, in other words, when the mean square error is minimized in all training experiments. The learning process was carried out employing the back propagation algorithm in conjugation with the Levenberg-Marquardt training function.

It is necessary to evaluate the performance of the network while training is underway. This is done using the validating data set, which contains 15% of the samples in our study. In the validating step, the goal is reaching the desirable error.

To test the performance of the trained network in training and validating processes, the experimental values were compared with the output of ANN. The correlation between

experimental data and training, and validating and testing sets, is depicted in Figs. 5 and 6. The perfect correlation (output exactly equal to target) is indicated by slope and y -intercept of the parity plot, equal to one and zero, respectively. The correlation coefficients (R value) for the training, validating, and testing sets were 0.987, 0.989, and 0.998, respectively, which demonstrated a good fit.

The MSE plot for all 17 samples is shown in Fig. 5d. As can be seen, the MSE of the network has a descending trend that indicates the network is learning. The best validation performance was at MSE of 471.11, obtained at epoch one.

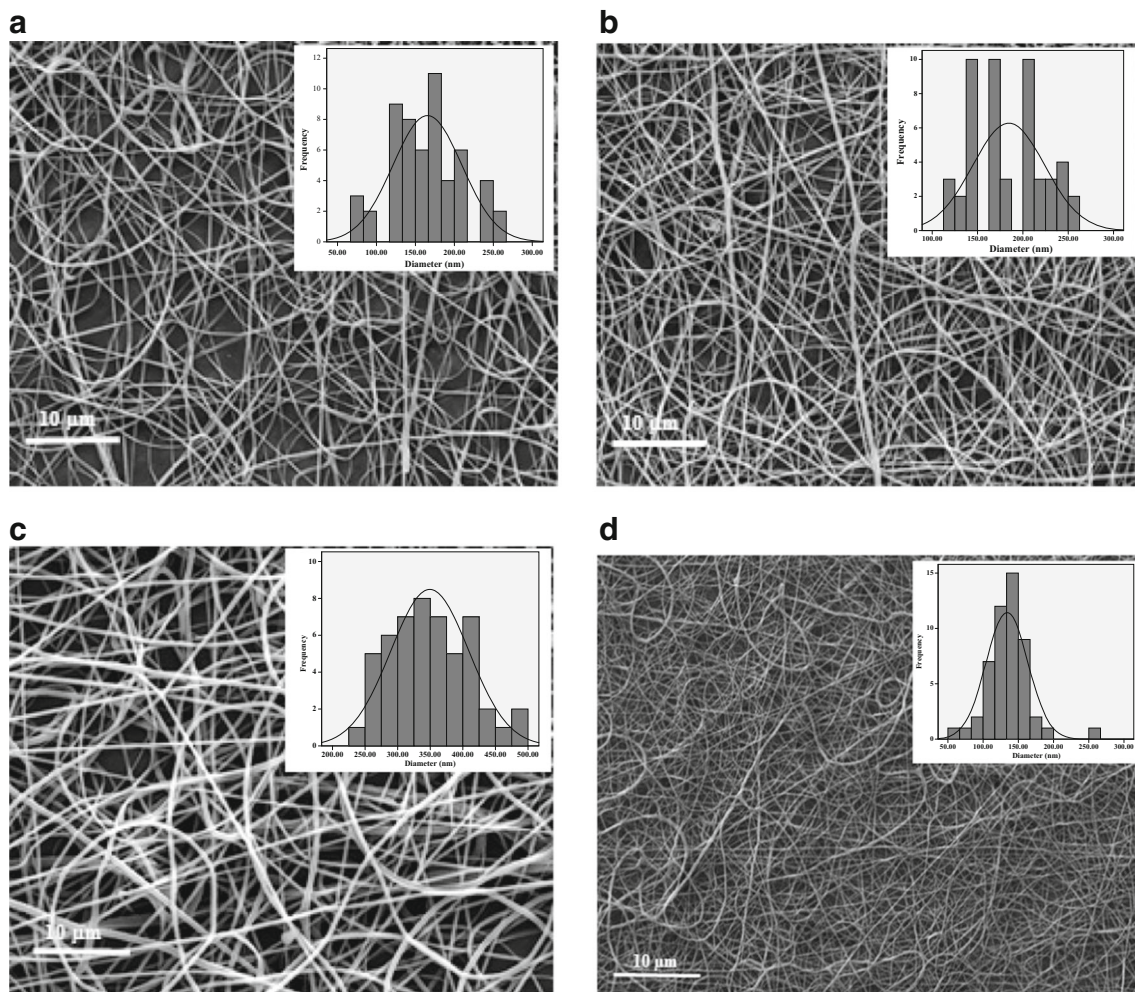


Fig. 7 SEM micrograph of electrospun PCL nanofiber and corresponding fiber diameter distribution. **a–c** Nanofibers from corresponding experiments in Table 4; **d** nanofibers at optimized condition (minimum diameter)

3.4 Comparison between RSM and ANN models

In this section, the aim is to determine which modeling technique shows better predictive accuracy. Hence, the experimental data and predicted values obtained via RSM and ANNs were compared to obtain the goodness of fitting. For this purpose, error analysis was carried out and R^2 , RMSE, MPE, and MAE were calculated according to the formulas mentioned in the previous section. As shown in Table 5, both models had good agreement with experimental data, which indicated by R^2 value, equal to 0.98 and 0.97 for RSM and ANN, respectively. The RSM model had slightly greater R^2 value and lower error than the ANN model (Fig. 6). This fact implied more predictive accuracy of RSM model. On the other hand, the ANN model itself provides little information about the input parameters and their contribution to the response if further analysis has not been done, whereas the main advantage of RSM is its ability to exhibit the factor contributions via coefficients in the regression model.

As the last step, to confirm the validity of the models, we carried out a validation study. Accordingly, additional experiments with different levels of input factors (polymer concentration, voltage, and distance) were conducted and the obtained responses were compared with predicted values. As shown in Table 6, there is no remarkable difference between experimental data and corresponding predicted values (Fig. 7a–c).

3.5 Optimization of electrospun PCL fiber

In a response surface optimization study, the objective is to find a desirable location in the design space. The demanded point could be a minimum, a maximum, or a special region where response is stable. In our study, the goal was to minimize the polymer diameter, which may provide maximum fiber surface area. The conditions for obtaining the finest PCL fiber diameter as determined by RSM model were polymer concentration = 8% (w/v), voltage = 15 kV, and distance = 8 cm.

Figure 7d shows the nanofiber morphology acquired in the optimized condition. The average fiber diameter was 129 nm, and the predicted fiber diameter under similar conditions estimated using RSM was 120 nm with a desirability value of 1. Comparison of the experimental value and the response provided by the model shows that the RSM model has an acceptable performance in the optimization study.

4 Conclusion

This paper presents a study on the effect of electrospinning variables including polymer concentration, voltage, and nozzle-to-collector distance on the average diameter of PCL nanofibers. Box-Behnken design has been carried out to create

minimum number of experiment needed for analysis of all the given parameters. RSM and ANN are applied in order to model and optimize nanofiber diameter. RSM analysis indicates that polymer concentration is the most effective factor on PCL fiber diameter.

Voltage and distance are in the next level of importance and the distance effect depends on the range of concentration. The optimum structure of ANN, based on the smallest MSE, is determined to be a three-layer network with Levenberg-Marquardt back-propagation learning algorithm, tangent sigmoid transfer function in the hidden layers containing 11 and 5 neurons, and linear transfer function in the output layer. The high regression coefficient between the experimental and predicted values reveals excellent evaluation of the data sets via the ANN and RSM models. Owing to the lower error of the RSM model, the performance of this model is better than that of the ANN model. In the optimization study, the condition for achieving the minimum diameter is defined. The observed diameter (129 nm) and the theoretical value predicted by RSM (120 nm) are very close, and the error percentage is very low. In addition, the validation study is performed as the last step to confirm the performance of both models. Overall, the collected results suggest that modeling techniques such as ANN and RSM can be useful tools for controlling the diameter of electrospun fibers, which is a key factor in determining properties of nanofibrous scaffolds.

Compliance with ethical standards

Conflict of interest The authors declare that they have no conflict of interest.

References

1. Woodruff MA, Hutmacher DW (2010) The return of a forgotten polymer—polycaprolactone in the 21st century. *Prog Polym Sci* 35(10):1217–1256
2. Alves da Silva M, Martins A, Costa-Pinto A, Costa P, Faria S, Gomes M, Reis R, Neves N (2010) Cartilage tissue engineering using electrospun PCL nanofiber meshes and MSCs. *Biomacromolecules* 11(12):3228–3236
3. Sinha V, Bansal K, Kaushik R, Kumria R, Trehan A (2004) Poly- ϵ -caprolactone microspheres and nanospheres: an overview. *Int J Pharm* 278(1):1–23
4. Ng KW, Achuth HN, Moochhala S, Lim TC, Hutmacher DW (2007) In vivo evaluation of an ultra-thin polycaprolactone film as a wound dressing. *J Biomater Sci Polym Ed* 18(7):925–938
5. Middleton JC, Tipton AJ (2000) Synthetic biodegradable polymers as orthopedic devices. *Biomaterials* 21(23):2335–2346
6. Freiberg S, Zhu X (2004) Polymer microspheres for controlled drug release. *Int J Pharm* 282(1):1–18
7. Gaucher G, Dufresne M-H, Sant VP, Kang N, Maysinger D, Leroux J-C (2005) Block copolymer micelles: preparation, characterization and application in drug delivery. *J Control Release* 109(1):169–188

8. Marrazzo C, Di Maio E, Iannace S (2008) Conventional and nanometric nucleating agents in poly (ϵ -caprolactone) foaming: crystals vs. bubbles nucleation. *Polym Eng Sci* 48(2):336–344
9. Lee K, Kim H, Khil M, Ra Y, Lee D (2003) Characterization of nano-structured poly (ϵ -caprolactone) nonwoven mats via electrospinning. *Polymer* 44(4):1287–1294
10. Hong S, Kim G (2011) Fabrication of size-controlled three-dimensional structures consisting of electrohydrodynamically produced polycaprolactone micro/nanofibers. *Applied Physics A* 103(4):1009–1014
11. Van de Witte P, Dijkstra P, Van den Berg J, Feijen J (1996) Phase separation processes in polymer solutions in relation to membrane formation. *J Membr Sci* 117(1):1–31
12. Chakarvarti S, Vetter J (1998) Template synthesis—a membrane based technology for generation of nano-/micro materials: a review. *Radiat Meas* 29(2):149–159
13. Teo W, Ramakrishna S (2006) A review on electrospinning design and nanofibre assemblies. *Nanotechnology* 17(14):R89
14. Andradý AL (2008) Science and technology of polymer nanofibers. John Wiley & Sons, Hoboken
15. Huang Z-M, Zhang Y-Z, Kotaki M, Ramakrishna S (2003) A review on polymer nanofibers by electrospinning and their applications in nanocomposites. *Compos Sci Technol* 63(15):2223–2253
16. Agarwal P, Mishra P, Srivastava P (2012) Statistical optimization of the electrospinning process for chitosan/poly(lactide) nanofabrication using response surface methodology. *J Mater Sci* 47(10):4262–4269
17. Doustgani A, Vashghani-Farahani E, Soleimani M, Hashemi-Najafabadi S (2012) Optimizing the mechanical properties of electrospun polycaprolactone and nanohydroxyapatite composite nanofibers. *Compos Part B* 43(4):1830–1836
18. Nasouri K, Bahrambeygi H, Rabbi A, Shoushtari AM, Kafrou A (2012) Modeling and optimization of electrospun PAN nanofiber diameter using response surface methodology and artificial neural networks. *J Appl Polym Sci* 126(1):127–135
19. Gunoglu K, Demir N, Akkurt I, Demirci ZN (2013) ANN modeling of the bremsstrahlung photon flux in tantalum target. *Neural Comput & Applic* 23(6):1591–1595
20. El-Shafie A (2014) Neural network nonlinear modeling for hydrogen production using anaerobic fermentation. *Neural Comput & Applic* 24(3–4):539–547
21. Sha W, Edwards K (2007) The use of artificial neural networks in materials science based research. *Mater Des* 28(6):1747–1752
22. Yördem O, Papila M, Menceloğlu YZ (2008) Effects of electrospinning parameters on polyacrylonitrile nanofiber diameter: an investigation by response surface methodology. *Mater Des* 29(1):34–44
23. Gu S, Ren J, Vancso G (2005) Process optimization and empirical modeling for electrospun polyacrylonitrile (PAN) nanofiber precursor of carbon nanofibers. *Eur Polym J* 41(11):2559–2568
24. Khanlou HM, Sadollah A, Ang BC, Kim JH, Talebian S, Ghadimi A (2014) Prediction and optimization of electrospinning parameters for polymethyl methacrylate nanofiber fabrication using response surface methodology and artificial neural networks. *Neural Comput & Applic* 25(3–4):767–777
25. Sadan MK, Ahn H-J, Chauhan G, Reddy N (2016) Quantitative estimation of poly (methyl methacrylate) nano-fiber membrane diameter by artificial neural networks. *Eur Polym J* 74:91–100
26. Sarkar K, Ghalia MB, Wu Z, Bose SC (2009) A neural network model for the numerical prediction of the diameter of electro-spun polyethylene oxide nanofibers. *J Mater Process Technol* 209(7):3156–3165
27. Rabbi A, Nasouri K, Bahrambeygi H, Shoushtari AM, Babaei MR (2012) RSM and ANN approaches for modeling and optimizing of electrospun polyurethane nanofibers morphology. *Fibers and Polymers* 13(8):1007–1014
28. Sarlak N, Nejad MAF, Shakheshi S, Shabani K (2012) Effects of electrospinning parameters on titanium dioxide nanofibers diameter and morphology: an investigation by Box–Wilson central composite design (CCD). *Chem Eng J* 210:410–416
29. Sadollah A, Ghadimi A, Metselaar IH, Bahreininejad A (2013) Prediction and optimization of stability parameters for titanium dioxide nanofluid using response surface methodology and artificial neural networks. *Sci Eng Compos Mater* 20(4):319–330
30. Faridi-Majidi R, Ziyadi H, Naderi N, Amani A (2012) Use of artificial neural networks to determine parameters controlling the nanofibers diameter in electrospinning of nylon-6,6. *J Appl Polym Sci* 124(2):1589–1597
31. Ali AA, Eltabey M, Farouk W, Zoalfakar SH (2014) Electrospun precursor carbon nanofibers optimization by using response surface methodology. *J Electrostat* 72(6):462–469
32. Gu SY, Ren J (2005) Process optimization and empirical modeling for electrospun poly (D,L-lactide) fibers using response surface methodology. *Macromol Mater Eng* 290(11):1097–1105
33. Naghibzadeh M, Adabi M (2014) Evaluation of effective electrospinning parameters controlling gelatin nanofibers diameter via modelling artificial neural networks. *Fibers and Polymers* 15(4):767–777
34. Khalili S, Khorasani SN, Saadatkish N, Khoshakhlagh K (2016) Characterization of gelatin/cellulose acetate nanofibrous scaffolds: prediction and optimization by response surface methodology and artificial neural networks. *Polymer Science Series A* 58(3):399–408
35. Gönen SÖ, Taygun ME, Küçükbayrak S (2015) Effects of electrospinning parameters on gelatin/poly (ϵ -caprolactone) nanofiber diameter. *Chemical Engineering & Technology* 38(5):844–850
36. Karimi MA, Pourhakkak P, Adabi M, Firoozi S, Adabi M, Naghibzadeh M (2015) Using an artificial neural network for the evaluation of the parameters controlling PVA/chitosan electrospun nanofibers diameter. *E-Polymers* 15(2):127–138
37. Ketabchi N, Naghibzadeh M, Adabi M, Esnaashari SS, Faridi-Majidi R (2016) Preparation and optimization of chitosan/polyethylene oxide nanofiber diameter using artificial neural networks. *Neural Computing and Applications*:1–13
38. Hsu CM, Shivkumar S (2004) N, N-Dimethylformamide additions to the solution for the electrospinning of poly (ϵ -caprolactone) nanofibers. *Macromol Mater Eng* 289(4):334–340
39. Chen M, Patra PK, Wamer SB, Bhowmick S (2007) Role of fiber diameter in adhesion and proliferation of NIH 3T3 fibroblast on electrospun polycaprolactone scaffolds. *Tissue Eng* 13(3):579–587
40. Box GE, Behnken DW (1960) Some new three level designs for the study of quantitative variables. *Technometrics* 2(4):455–475
41. Manohar M, Joseph J, Selvaraj T, Sivakumar D (2013) Application of Box Behnken design to optimize the parameters for turning Inconel 718 using coated carbide tools. *International Journal of Scientific & Engineering Research* 4(4):620–642
42. Bölgen N, Menceloğlu YZ, Acatay K, Vargel I, Pişkin E (2005) In vitro and in vivo degradation of non-woven materials made of poly (ϵ -caprolactone) nanofibers prepared by electrospinning under different conditions. *J Biomater Sci Polym Ed* 16(12):1537–1555
43. Hornik K, Stinchcombe M, White H (1989) Multilayer feedforward networks are universal approximators. *Neural Netw* 2(5):359–366
44. Keecman V (2001) Learning and soft computing: support vector machines, neural networks, and fuzzy logic models. MIT Press, Cambridge
45. Wang L, Fu X (2006) Data mining with computational intelligence. Springer Science & Business Media, Berlin
46. Fu X, Wang L (2003) Data dimensionality reduction with application to simplifying RBF network structure and improving classification performance. *IEEE Transactions on Systems, Man, and Cybernetics, Part B (Cybernetics)* 33(3):399–409